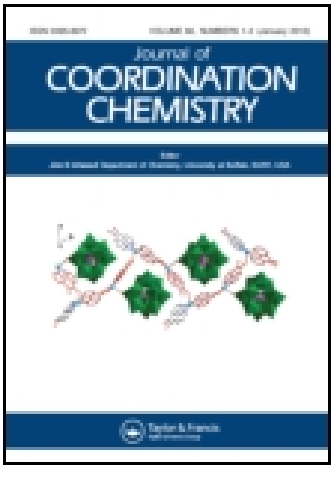

Journal of Coordination Chemistry
Publication details, including instructions for authors and subscription information:
http://www.tandfonline.com/loi/gcoo20

Metal-organic polymers of Sr(II) and Ce(IV): structural studies, supramolecular synthons, and potentiometric measurements

Mohammad Ghadermazi[a], Shabnam Sheshmani[b], Ardeshir Shokrollahi[c] & Jeiran Karami Arokhloo[d]

[a] Faculty of Science, Department of Chemistry, University of Kurdistan, Sanandaj, Iran

[b] Department of Chemistry, College of Basic Sciences, Yadegar-e-Imam Khomeini (RAH) Branch, Islamic Azad University, Tehran, Iran

[c] Department of Chemistry, Yasouj University, Yasouj, Iran

[d] Department of Chemistry, Gachsaran Branch, Islamic Azad University, Gachsaran, Iran

Accepted author version posted online: 23 Sep 2014.Published online: 07 Oct 2014.

To cite this article: Mohammad Ghadermazi, Shabnam Sheshmani, Ardeshir Shokrollahi & Jeiran Karami Arokhloo (2014) Metal-organic polymers of Sr(II) and Ce(IV): structural studies, supramolecular synthons, and potentiometric measurements, Journal of Coordination Chemistry, 67:21, 3492-3509, DOI: 10.1080/00958972.2014.966101

To link to this article: http://dx.doi.org/10.1080/00958972.2014.966101

Journal of Coordination Chemistry, 2014
Vol. 67, No. 21, 3492–3509, http://dx.doi.org/10.1080/00958972.2014.966101

Metal–organic polymers of Sr(II) and Ce(IV): structural studies, supramolecular synthons, and potentiometric measurements

MOHAMMAD GHADERMAZI*†, SHABNAM SHESHMANI‡, ARDESHIR SHOKROLLAHI§ and JEIRAN KARAMI AROKHLOO¶

†Faculty of Science, Department of Chemistry, University of Kurdistan, Sanandaj, Iran
‡Department of Chemistry, College of Basic Sciences, Yadegar-e-Imam Khomeini (RAH) Branch, Islamic Azad University, Tehran, Iran
§Department of Chemistry, Yasouj University, Yasouj, Iran
¶Department of Chemistry, Gachsaran Branch, Islamic Azad University, Gachsaran, Iran

(*Received 6 January 2014; accepted 21 August 2014*)

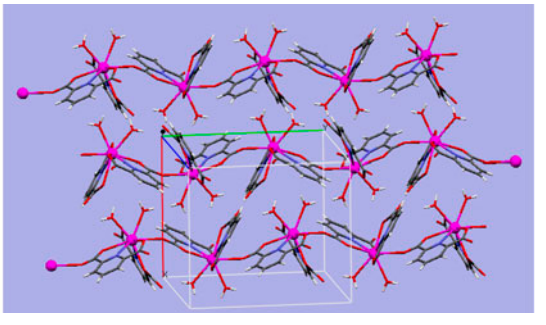

Two metal–organic coordination polymers based on a salt, $(pydcH)_3 \cdot (pipzH_2)_{1.5} \cdot (H_2O)_{3.7}$, between pyridine-2,6-dicarboxylic acid, $pydcH_2$, and piperazine, pipz, formulated as $(pipzH_2)[Sr(pydc)_2(H_2O)_2]_n \cdot 4H_2O$ and $[Ce(pydc)_2(H_2O)_2]_n \cdot 4H_2O$ were prepared. The synthesis, IR spectroscopy, elemental analysis, single-crystal X-ray diffraction, supramolecular synthons, and potentiometric measurements were investigated. The chemical environment around each Sr(II) or Ce(IV) was a distorted tricapped trigonal prism. The butterfly- and ladder-like structures of these complexes were bridged by oxygens of $(pydc)^{2-}$ and M–O(pydc)–M bonds. In the crystal structure, intermolecular O–H···O, N–H···O, and C–H···O hydrogen bonds result in the formation of supramolecular structures. The stoichiometry and stability of the pydc–pipz system with Sr(II) in aqueous solution were investigated by potentiometric titration. The stoichiometry of complex species in solution was found to be similar to the cited crystalline metal ion complexes.

Keywords: Strontium (II); Cerium (IV); Pyridine-2,6-dicarboxylic acid; Piperazine; Coordination polymer; Solution studies

*Corresponding author. Email: mghadermazi@uok.ac.ir

1. Introduction

A variety of factors can influence the self-assembly of coordination frameworks making desired topologies and specific properties a difficult challenge [1–5]. Construction of coordination polymers with new network motifs is of interest for the development of new functional materials and in fundamental studies of crystal engineering and supramolecular chemistry [6–13]. Assembly of metal–organic frameworks may provide a new strategy for achieving solid functional materials with the application in molecular absorption/separation, magnetism, ion exchange, electric conductivity, catalysis, etc. [14, 15]. Self-assembly for coordination polymers is a useful method due to the following reasons: (1) A wide variety of frameworks can be realized from simple building blocks of metals, organic ligands such as carboxylic acid and counter cation; (2) modification of organic ligand is possible; and (3) interactions such as M–M bond and van der Waals interactions are available. Insight into these structures involve investigation of van der Waals, ion-pairing, hydrogen bonding, face-to-face π–π stacking, and edge-to-face C–H$\cdots\pi$, C–O$\cdots\pi$, N–H$\cdots\pi$, S–O$\cdots\pi$, Ti$\cdots\pi$, Hg–Cl$\cdots\pi$, S$\cdots$S interactions in the crystal lattice. Carboxylates have various coordination modes, leading to the formation of mononuclear, binuclear, and polymeric compounds. Recently, building blocks with heterocyclic acids, such as pyridine, pyrazole, and imidazole carboxylic acids, have been used in the construction of coordination polymers with 1-, 2-, and 3-D networks [16–18]. The growing interest in the coordination chemistry of s-block and lanthanide elements has been demonstrated by several recent reviews. Compared to the extensive chemistry of coordination polymers based on transition metals, the coordination chemistry of group two metals with organic linkers such as 2-thiobarbituric acid [19], pyridine 2,4,6-tricarboxylate [20], and barium 1,3-propanediaminetetraacetates [21] is less explored. Also, the coordination chemistry of cerium with ligands such as 1,4-benzene dicarboxylic acid [22], pyridine-2,4,6-tricarboxylic acid [23], and 3,4-pyrazoledicarboxylic acid [24] has been studied.

In this research, we report the synthesis, structural behavior, and potentiometric studies of two metal–organic coordination polymers obtained from a salt between pyridine-2,6-dicarboxylic acid and piperazine.

2. Experimental

2.1. *Reagents and apparatus*

All chemicals used were of commercial suppliers and used without purification. Doubly distilled deionized water was used as needed. Melting points were determined with an Electrothermal IA-9100 and were not corrected. IR spectra were recorded on an 843 Perkin-Elmer spectrophotometer using KBr disks. Elemental analyses (C, H, and N) were carried out with a Perkin-Elmer 2400 CHN elemental analyzer.

2.2. *Crystallographic data collection and structure determination*

Single-crystal data were collected at 100(2) K on a Bruker SMART APEX II CCD area-detector diffractometer equipped with sealed-tube graphite-monochromated Mo-Kα radiation $\lambda = 0.71073$ Å. Programs used for cell refinement and data reduction were *APEX2*, Bruker, 2005 [25]. Also, programs used to solve and refine the structures were *SHELXTL*

ver. 5.1, Sheldrick, 1998, and *SHELXTL* ver. 5.1, Sheldrick, 1998, respectively. Software used for molecular graphics was *SHELXTL* ver. 5.1, Sheldrick, 1998 [26].

In the Sr(II) complex, hydrogens of NH_2 and water were found in different Fourier synthesis. The H(C) positions were calculated. All hydrogens were refined in isotropic approximation within riding model with the U_{iso}(H) parameters equal to 1.2 U_{eq}(Ci), 1.2 U_{eq}(Nj), and 1.5 U_{eq}(Oj), where U(Ci), U(Nj), and U(Oj) are the equivalent thermal parameters of the carbon, nitrogen, or oxygen atoms to which corresponding hydrogens are bonded.

In the Ce(IV) complex, the positions of H(C) atoms were calculated and H(O) atoms were found from different Fourier maps. All hydrogens were treated in riding model with the U_{iso}(H) parameters equal to 1.2 U_{eq}(Ci) and 1.5(Oi), where U_{eq}(X) are the equivalent thermal parameters of the atoms to which corresponding hydrogens are bonded.

2.3. *Potentiometric equilibrium measurements*

A Model 794 Metrohm Basic Titrino was attached to an extension-combined glass–calomel electrode mounted in an air-protected, sealed, thermostated jacketed cell maintained at 25.0 ± 0.1 °C by circulating water, from a constant-temperature bath Fisherbrand model FBH604, LAUDA, Germany, equipped with a stirrer and a 10.000 mL-capacity Metrohm piston burette. The pH meter–electrode system was calibrated to read –log [H^+].

2.4. *Potentiometric procedure*

The details are described [27–30]. The concentrations of pipz and pydc were 2.50×10^{-3} M for the potentiometric pH titrations of pydc, pipz, and pydc–pipz, in the absence and presence of 1.25×10^{-3} M Sr^{2+} ion. A standard carbonate-free NaOH solution (0.105910 M) was used in all titrations. The ionic strength was adjusted to 0.1 M with $NaNO_3$. Before an experimental point (pH) was measured, sufficient time was allowed for the establishment of equilibrium. Protonation constants of ligands, stability constants of salt, and its metal ion complex were evaluated using the BEST program described by Martell and Motekaitis [31]. The value of $K_w = [H^+][OH^-]$ was used in the calculations according our previous work [27–29].

2.5. *Synthesis of salt compound*

The synthetic procedure of proton transfer compound was described elsewhere [32]. In brief, to a solution of pyridine-2,6-dicarboxylic acid (1.67 g, 10 mM) in methanol (100 mL) was added piperazine (0.86 g, 10 mM) in methanol (10 mL). The precipitate was filtered off and dried. The crude product (0.5 g) was recrystallized from water (10 mL). Prism yellow crystals of this compound were obtained from the clear solution by slow evaporation of the filtrate at room temperature after ten days. m.p.: 273 °C, yield: 92.54%.

2.6. *Synthesis of Sr(II) coordination polymer, 1*

A solution of $SrCl_2 \cdot 6H_2O$ (1 mM, 0.266 g) in water (10 mL) was added to a solution of salt compound (3 mM) in water (10 mL). The adopted synthesis procedure is shown in scheme 1. The resulting solution was stirred for one hour. The prism colorless crystals were isolated from the clear solution after 10 days. m.p.: decomposed at 400 °C, IR (KBr): 3600–3000 (s),

2643 (w), 1680–1700 (s), 1676 (s), 1619 (w), 1586 (s), 1548 (s), 1452 (s), 1439 (s), 1385 (s), 1354 (m), 1318 (w), 1211 (w), 1178 (m), 1165 (m), 1083 (s), 1001 (s), 880 (m), 851 (m), 802 (m), 759 (s), 740 (s), 675 (s), 644 (s), 599 (w), 490 (w), 423 (m), and 339 (w) cm^{-1}. Found (%): C, 35.07; H, 4.67; and N, 9.11. Calcd for $C_{18}H_{30}N_4O_{14}Sr$ (614.08) (%): C, 35.17; H, 4.88; and N, 9.12.

2.7. *Synthesis of Ce(IV) coordination polymer, 2*

Complex **2** was obtained by a similar method to that used for preparation of **1,** but ammonium cerium(IV) nitrate (0.548 g, 1 mM) was used instead of $SrCl_2 \cdot 6H_2O$. The synthesis procedure is shown in scheme 2. After slow evaporation of the solvent at room temperature, prism yellow single crystals of **2** were obtained after five days. m.p.: Decomposed at 400 °C, IR (KBr): 3571–3110 (s), 3088 (m), 3053 (m), 1700 (s), 1685 (s), 1661 (s), 1653 (s), 1643 (s), 1633 (s), 1597 (m), 1556 (w), 1578 (m), 1473 (w), 1430 (m), 1377 (m), 1356 (s), 1349 (s), 1264 (w), 1175 (m), 1098 (m), 1087 (w), 1037 (m), 914 (m), 867 (w), 835 (w), 789 (m), 757 (m), 740 (s), 691 (m), 678 (m), 598 (w), 456 (w), 406 (w), 341 (w), 313 (w), and 273 (m) cm^{-1}. Found (%): C, 29.00; H, 3.08; and N, 4.75. Calcd for $C_{14}H_{18}CeN_2O_{14}$ (578.42) (%): C, 29.04; H, 3.11; and N, 4.84.

3. Results and discussion

3.1. *Infrared spectrum of 1 and 2*

The IR spectra of **1** and **2** were recorded from 400 to 4000 cm^{-1}. The characteristic peaks of these compounds were observed. For example, peaks at 3600–3200 cm^{-1} are attributed to C–H, N–H, and O–H stretches of piperazinediium, pyridine-2,6-dicarboxylate, and crystallization waters of the lattice [33]. The peaks at 1700 and 1500 cm^{-1} are attributed to asymmetric and symmetric stretching vibrations of carboxylates, respectively [34]. Complexes **1** and **2** were synthesized by reaction of $(pydcH)_3 \cdot (pipzH_2)_{1.5} \cdot (H_2O)_{3.7}$ ion pair with Sr(II) and Ce(IV) salt in 3 : 1 M ratio. The most diagnostic IR bands of these complexes correspond to the stretching vibration of carboxyl in the expected regions. The bands at 1680–1700 cm^{-1} are attributed to carboxylate groups in **1** and **2**. The separation ($\Delta\nu$) between $\nu_{as}(COO^-)$ and $\nu_s(COO^-)$ has been often used to diagnose the coordination modes in carboxylate ligands. The separation for unidentate carboxylato groups is >200 cm^{-1}, whereas it is <200 cm^{-1} in multidentate ones [35]. Strong characteristic bands of the carboxyl groups are observed at 1680–1700 cm^{-1} for the asymmetric vibrations and 1580 cm^{-1} for symmetric vibrations, respectively. Thus, in **1** and **2**, the $\Delta\nu$ value is 120 cm^{-1}, suggesting multibinding of the carboxylate to metal ions. In all compounds, the δ(O–C–O) in plane deformation vibration occurs at 740 cm^{-1} [36]. Prominent bands of 1586 and 1578 cm^{-1} in **1** and **2** are typical of scissoring NH vibrations, and medium peaks at 1370–1590 cm^{-1} are due to aromatic C=C bonds. Finally, 1180 cm^{-1} is attributed to the stretching mode of C–N bonds. Another feature of the IR spectrum is a broad band centered at 3306 cm^{-1} due to ν_{OH} of coordinated and/or crystallization water. The feature at 1600 cm^{-1} is from bending H–O–H frequency [37, 38]. In general, the infrared spectra and elemental analyses of **1** and **2** are fully consistent with their structural characteristics as determined by single-crystal X-ray diffraction.

3.2. *Crystal and molecular structure of $(pipzH_2)[Sr(pydc)_2(H_2O)_2]_n{\cdot}4H_2O$, 1*

The procedure adopted in the synthesis of $(pipzH_2)[Sr(pydc)_2(H_2O)_2]_n{\cdot}4H_2O$ is outlined in scheme 1. The reaction of $SrCl_2{\cdot}6H_2O$ with $(pydcH)_3{\cdot}(pipzH_2)_{1.5}{\cdot}(H_2O)_{3.7}$ in aqueous solution leads to the formation of this polymeric complex. A view of the molecular structure of $(pipzH_2)[Sr(pydc)_2(H_2O)_2]_n{\cdot}4H_2O$ is shown in figure 1. Also, polymeric chain diagram in butterfly-like structure in the unit cell is shown in figure 2. A summary of crystallographic data is given in table 1. Selected distances and angles are presented in table 2. Also, a list of intra- and intermolecular hydrogen bonds is given in table 3.

This complex crystallizes in monoclinic $P2_1/n$ space group with four molecules in the unit cell. In the preparation of the complex, we used $(pydcH)_3{\cdot}(pipzH_2)_{1.5}{\cdot}(H_2O)_{3.7}$ containing proton donor and proton acceptor, similar to the result, which proved that $(pydc)^{2-}$ and $(pipzH_2)^{2+}$ have contributed to the molecular structure, forming a 2-D coordination polymer. The piperazinediium molecules did not incorporate in the coordination although they were a cationic counter ion.

In the crystal structure, $Sr^{II}(1)$ is coordinated by two nitrogens and four oxygens of two pyridine-2,6-dicarboxylates by two waters and also by one oxygen of $(pydc)^{2-}$ which acts as a bridge (figure 1). Therefore, in **1**, Sr(1) is coordinated in a distorted tricapped trigonal

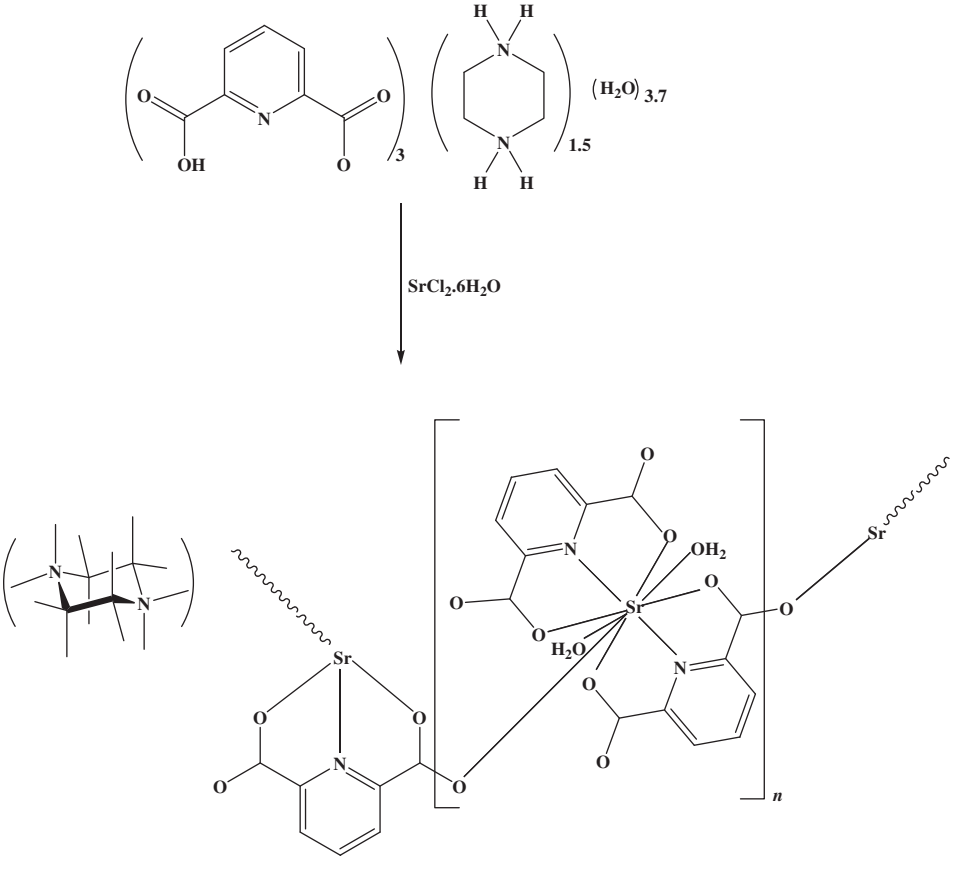

Scheme 1. Synthetic procedure for $(pipzH_2)[Sr(pydc)_2(H_2O)_2]_n$.

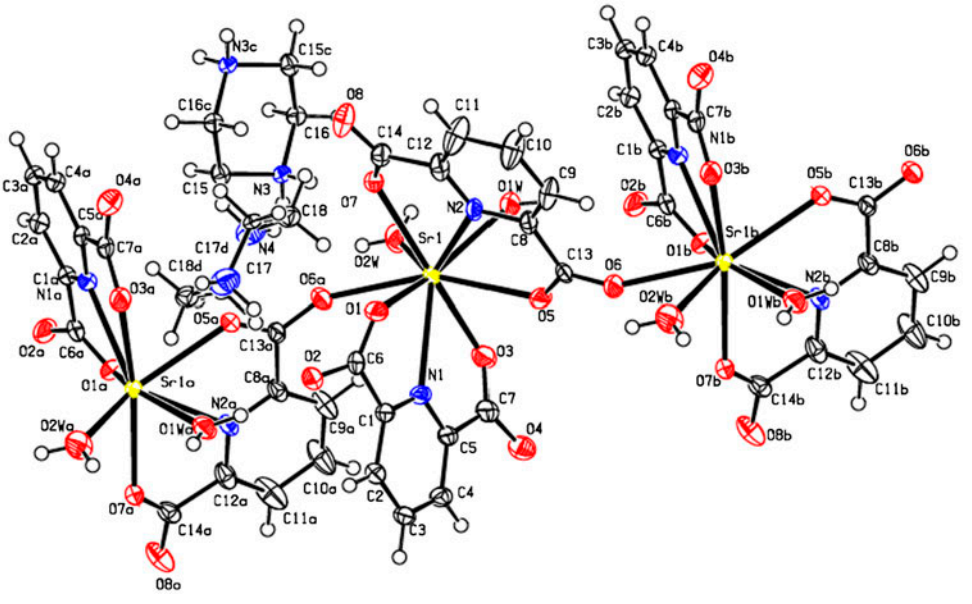

Figure 1. A view of the molecular structure of $(pipzH_2)[Sr(pydc)_2(H_2O)_2]_n \cdot 4H_2O$, showing the atom numbering scheme.

prism coordination geometry (nine-coordinate), with O(1), O(3), O(5), O(6), O(7), and O (1W) forming one trigonal prism, and O(2W), N(1), and N(2) forming three caps (figure 3). The two Sr(1)–N(1) and Sr(1)–N(2) distances are 2.744(4) and 2.669(4) Å and the seven Sr (1)–O distances are 2.577(4)–2.746(4) Å (table 2). As can be seen from figures 1 and 2, Sr^{II}–O(pydc)–Sr^{II} are rungs of the butterfly-like structure, which are alternately repeated in the crystalline network. In this polymeric complex, pyridine-2,6-dicarboxylate bridges two Sr(II) ions. The units are then linked into an infinite system via additional Sr–pydc bonds.

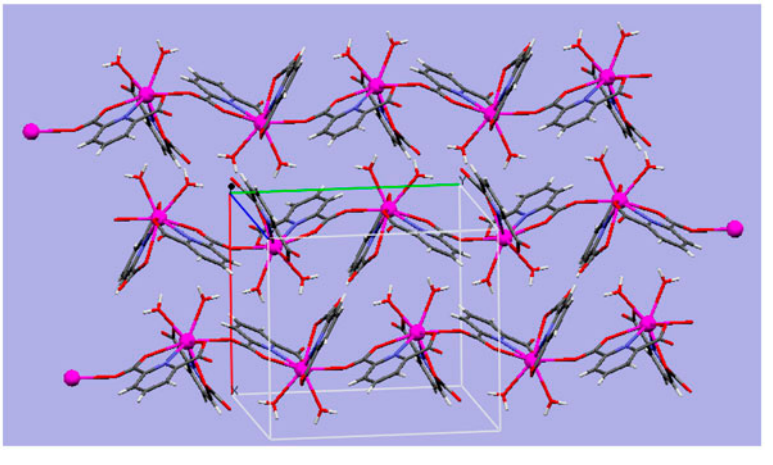

Figure 2. Polymeric chain in butterfly like structure for **1**. Water molecules and piperazinediium are omitted for clarity.

Table 1. Crystallography and parameters for the data collection and refinements for **1** and **2**.

Crystal data	**1**	**2**
Empirical formula	$C_{18}H_{30}N_4O_{14}Sr$	$C_{14}H_{18}CeN_2O_{14}$
Formula weight	614.08	578.42
Crystal system	Monoclinic	Monoclinic
Space group	$P2_1/n$ $Z = 4$	$P\ 2_1/c$ $Z = 4$
Hall symbol	*–P2yn*	*–P2ybc*
Unit cell dimensions	$a = 11.995(2)$ Å	$a = 14.002(6)$ Å
	$b = 13.701(2)$ Å, $\beta = 90.098(3)°$	$b = 11.225(5)$ Å, $\beta = 102.193(1)°$
	$c = 15.143(2)$ Å	$c = 12.954(6)$ Å
D_x (Mgm^{-3})	1.639	1.931
V (Å^3)	2488.7(6)	1990.0(2)
Absorption coefficient (mm^{-1})	2.243	2.365
Crystal dimensions (mm^3)	0.20 × 0.20 × 0.15	0.18 × 0.11 × 0.07
Crystal shape and color	Prism, colorless	Prism, yellow
F (000)	1264	1144
θ Range for data collection (°)	2.16–25.67, θ_{min}, θ_{max} = 2.0–27.0°	2.42–34.20, θ_{min}, θ_{max} = 2.4–30.0°
Index ranges	$-15 \le h \le 15$	$-19 \le h \le 19$
	$-17 \le k \le 17$	$-15 \le k \le 15$
	$-19 \le l \le 19$	$-18 \le l \le 18$
No. of reflections for cell parameters	4932	4749
Measured reflections	31,533	25,000
Independent reflections	5336	5808
Reflections with $I > 2\sigma(I)$	3936	5411
No. of parameters	352	278
Goodness of fit on F^2	0.948	1.004
Final R indices [$I > 2\sigma(I)$]	$R_1 = 0.0593$, $wR_2 = 0.1294$	$R_1 = 0.0263$, $wR_2 = 0.0779$
R indices (all data)	$R_1 = 0.0877$, $wR_2 = 0.1455$	$R_1 = 0.0295$, $wR_2 = 0.0809$
Largest diff. peak and hole (e Å^{-3})	–0.84–1.64	–1.57–1.07

Intermolecular hydrogen-bond interactions and Sr–pydc–Sr distances have essential roles in creation of the 2-D supramolecular structure of **1**. Hydrogen bonds play an important role in the stabilization of supramolecular systems both in solution and in the solid state and there is clearly a need for better understanding of how such aggregates influence the overall structure. In this structure, oxygens of carboxylate groups, coordinated water, and co-crystallized water, are held together by hydrogen bonds (figure 4). This hydrogen bonding

Table 2. Selected distances (Å) and angles (°) of $(pipzH_2)[Sr(pydc)_2(H_2O)_2]_n \cdot 4H_2O$.

Sr(1)–O(1)	2.746(4)	Sr(1)–O(6)	2.568(3)	Sr(1)–O(2W)	2.647(4)
Sr(1)–O(3)	2.597(4)	Sr(1)–O(7)	2.577(4)	Sr(1)–N(1)	2.744(4)
Sr(1)–O(5)	2.621(4)	Sr(1)–O(1W)	2.663(4)	Sr(1)–N(2)	2.669(4)
O(1)–Sr(1)–O(3)	118.48(11)	O(3)–Sr(1)–O(2W)	80.58(12)	O(6)–Sr(1)–N(1)	76.18(12)
O(1)–Sr(1)–O(5)	92.96(12)	O(3)–Sr(1)–N(1)	59.87(12)	O(6)–Sr(1)–N(2)	126.92(13)
O(1)–Sr(1)–O(6)	71.06(12)	O(3)–Sr(1)–N(2)	130.93(12)	O(7)–Sr(1)–O(1W)	89.09(12)
O(1)–Sr(1)–O(7)	76.09(11)	O(5)–Sr(1)–O(6)	155.17(12)	O(7)–Sr(1)–O(2W)	82.08(12)
O(1)–Sr(1)–O(1W)	150.60(12)	O(5)–Sr(1)–O(7)	120.70(12)	O(7)–Sr(1)–N(1)	132.26(13)
O(1)–Sr(1)–O(2W)	135.80(11)	O(5)–Sr(1)–O(1W)	72.76(12)	O(7)–Sr(1)–N(2)	60.58(12)
O(1)–Sr(1)–N(1)	58.89(12)	O(5)–Sr(1)–O(2W)	131.13(13)	O(1W)–Sr(1)–O(2W)	64.48(13)
O(1)–Sr(1)–N(2)	71.46(11)	O(5)–Sr(1)–N(1)	79.29(12)	O(1W)–Sr(1)–N(1)	138.25(13)
O(3)–Sr(1)–O(5)	70.57(12)	O(5)–Sr(1)–N(2)	60.70(12)	O(1W)–Sr(1)–N(2)	79.15(13)
O(3)–Sr(1)–O(6)	99.84(12)	O(6)–Sr(1)–O(7)	74.87(12)	O(2W)–Sr(1)–N(1)	118.80(13)
O(3)–Sr(1)–O(7)	162.53(12)	O(6)–Sr(1)–O(1W)	129.79(12)	O(2W)–Sr(1)–N(2)	128.00(13)
O(3)–Sr(1)–O(1W)	81.59(12)	O(6)–Sr(1)–O(2W)	66.31(12)	N(1)–Sr(1)–N(2)	113.12(12)

Table 3. Intra- and intermolecular hydrogen bonds for $(pipzH_2)[Sr(pydc)_2(H_2O)_2]_n \cdot 4H_2O$.

D–H	A	d(D–H)	d(H···A)	d(D···A)	<DHA	Symmetry codes
N(3)–H(3N1)	O(4W)	0.90	1.950	2.822(6)	163	
N(3)–H(3N1)	O(6)	0.90	2.560	2.959(5)	107	$-x+1/2, y-1/2, -z-1/2$
N(3)–H(3N2)	O(7)	0.90	1.836	2.722(6)	168	
N(4)–H(4N2)	O(4)	0.90	2.590	3.325(7)	139	$-x+1/2, y-1/2, -z-1/2$
O(1W)–H(1W1)	O(3W)	0.85	1.996	2.838(6)	170	
O(1W)–H(1W2)	O(2)	0.85	2.005	2.805(6)	156	$-x+1/2, y+1/2, -z-1/2$
O(2W)–H(2W1)	O(3W)	0.85	2.390	3.130(7)	146	
O(2W)–H(2W1)	O(6WA)	0.85	2.208	2.952(8)	146	$x+1/2, -y+1/2, z-1/2$
O(2W)–H(2W2)	O(4W)	0.85	1.935	2.773(6)	168	
O(3W)–H(3W1)	O(8)	0.85	1.850	2.680(6)	165	$x+1/2, -y+1/2, z+1/2$
O(3W)–H(3W2)	O(6WA)	0.85	1.703	2.514(8)	159	$x+1/2, -y+1/2, z-1/2$
O(4W)–H(4W1)	O(6WB)	0.85	2.132	2.967(1)	167	$x+1/2, -y+1/2, z-1/2$
O(4W)–H(4W2)	O(5WB)	0.85	1.658	2.489(1)	165	$-x+1, -y, -z$
O(4W)–H(4W2)	O(5WA)	0.85	1.993	2.831(8)	169	$-x+1, -y, -z$
O(5WA)–H(5W1)	O(1)	0.85	2.019	2.854(8)	167	$x+1/2, -y+1/2, z+1/2$
O(5WA)–H(5W2)	O(4)	0.85	2.052	2.827(8)	151	
O(5WB)–H(5W3)	O(3W)	0.85	2.510	3.173(1)	136	$x–1/2, –y+1/2, z+1/2$
O(5WB)–H(5W3)	O(4)	0.85	2.273	2.707(1)	112	
O(5WB)–H(5W3)	O(6WA)	0.85	2.250	3.031(1)	152	
O(5WB)–H(5W4)	O(4)	0.85	2.020	2.707(1)	137	
O(6WA)–H(6W1)	O(4)	0.85	1.737	2.562(8)	163	
O(6WA)–H(6W1)	O(5WB)	0.85	2.520	3.031(1)	120	
O(6WA)–H(6W2)	O(2)	0.85	2.155	2.989(8)	167	$x+1/2, -y+1/2, z+1/2$
O(6WB)–H(6W3)	O(4W)	0.85	2.320	2.967(1)	134	$x-1/2, -y+1/2, z+1/2$
O(6WB)–H(6W4)	O(2)	0.85	1.873	2.561(10)	137	$x+1/2, -y+1/2, z+1/2$
C(15)–H(15A)	O(5)	0.99	2.49	3.384(7)	150	$1/2-x, -1/2+y, -1/2-z$
C(16)–H(16A)	O(8)	0.99	2.54	3.440(7)	151	$1-x, -y, -1-z$
C(17)–H(17A)	O(2)	0.99	1.79	2.774(6)	171	
C(17)–H(17B)	O(3)	0.99	1.86	2.741(6)	147	$1/2-x, -1/2+y, -1/2$
C(17)–H(17B)	O(5)	0.99	2.53	2.230(7)	127	$1/2-x, -1/2+y, -1/2$
C(18)–H(18B)	O(8)	0.99	2.51	3.242(6)	131	

interaction can result in the formation of diverse contacts. By considering the crystalline network of **1**, there are three types of interactions with $R_4^3(10)$, $R_3^3(8)$, and $C_4^4C_4^4(10)$. Also, spatial arrangement of interacting fragments in Type I and II hydrogen bonds are shown in figure 4.

Piperazine as an organic base is easily protonated in acidic solution, forming $(pipzH_2)^{2+}$; $(pipzH_2)^{2+}$ ions in a chair configuration are excellent hydrogen-bond donors [39–41] and at the same time provide counter-charge. The hydrogen bonds between $(pipzH_2)^{2+}$ and anionic complex (table 3) lead to a cyclic motif $R_2^2(6)$ (figure 5). Extended network forms via N–H···O hydrogen bonds between the piperazinediium and oxygens of carboxylate groups in the polymeric chain (figure 5).

In the crystal structure, C–H···π stacking was observed between C(9)–H(9A) and pyridine rings (N1, C1–C5), with distance of 3.652 Å and angle of 86.36° (figure 6).

3.3. *Crystal and molecular structure of $[Ce(pydc)_2(H_2O)_2]_n \cdot 4H_2O$, 2*

Synthesis of **2** is shown in scheme 2. Crystallography and parameters for the data collection and refinement are given in table 1. Selected bond distances and angles together with intra- and intermolecular hydrogen bonds are listed in tables 4 and 5.

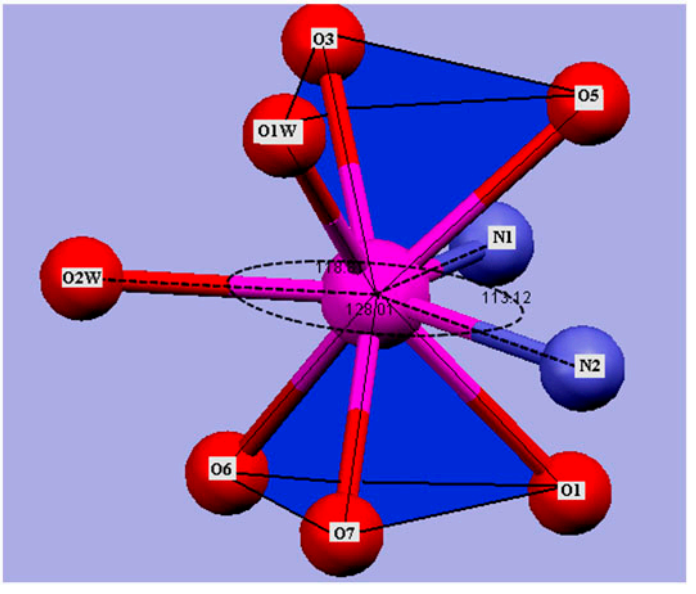

Figure 3. Representation of the coordination environment around Sr^{2+} as distorted tricapped trigonal prism with coordination number nine.

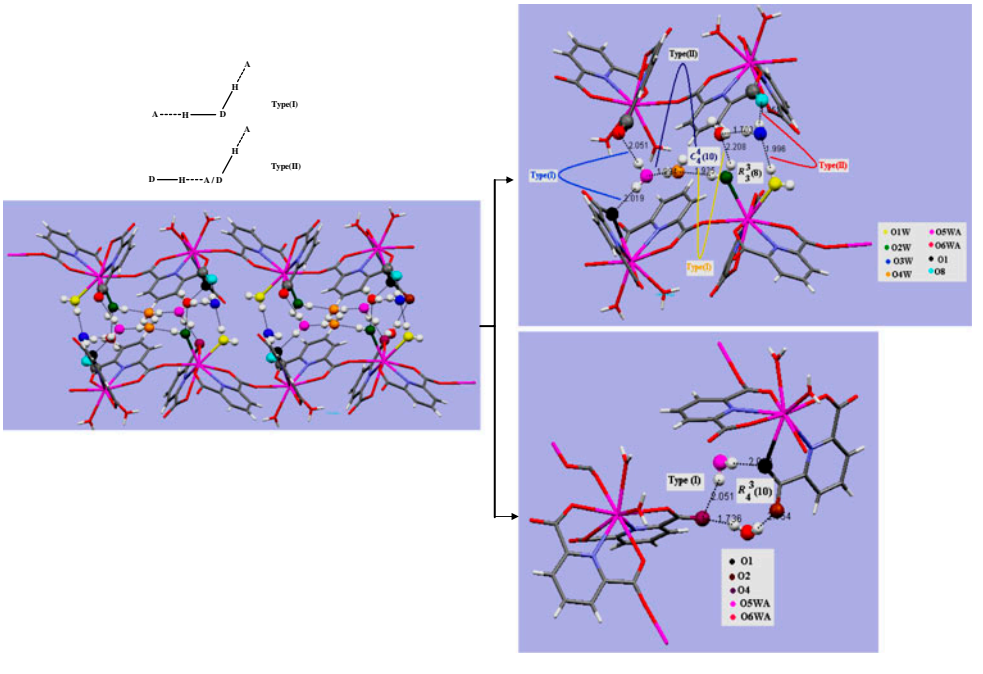

Figure 4. Schematic representation of the hydrogen bonding cyclic and chain motifs $R_4^3(10)$, $R_3^3(8)$ and $C_4^4(10)$ determined by O–H···O bonds between water and $(pydc)^{2-}$ fragments in **1**. Spatial arrangement of interacting fragments in Type I and II hydrogen bonds. D and A denote donor and acceptor sites.

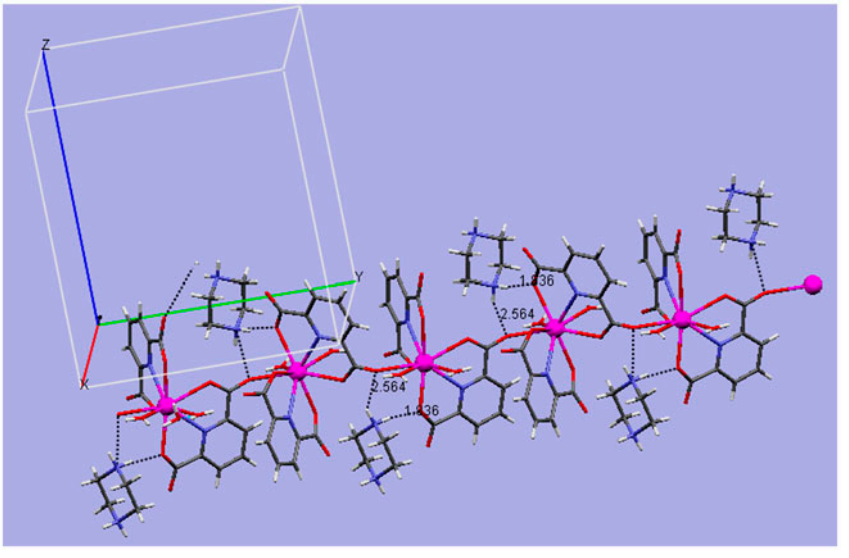

Single-crystal X-ray diffraction analyses showed that **2** exhibits a 3-D polymeric structure, made from $[Ce(pydc)_2(H_2O)_2]$ (figure 7). Based upon the molecular structure analysis of the neutral polymeric complex, one finds that Ce(IV) centers reside in a distorted tricapped trigonal prism coordination environment with coordination number nine by two nitrogens and four oxygens of two $(pydc)^{2-}$, two waters and one oxygen of $(pydc)^{2-}$ (figures 7 and 8). In fact, the summation of O(8)–Ce–N(1), O(8)–Ce–N(2), and N(1)–Ce–N(2) angles in the

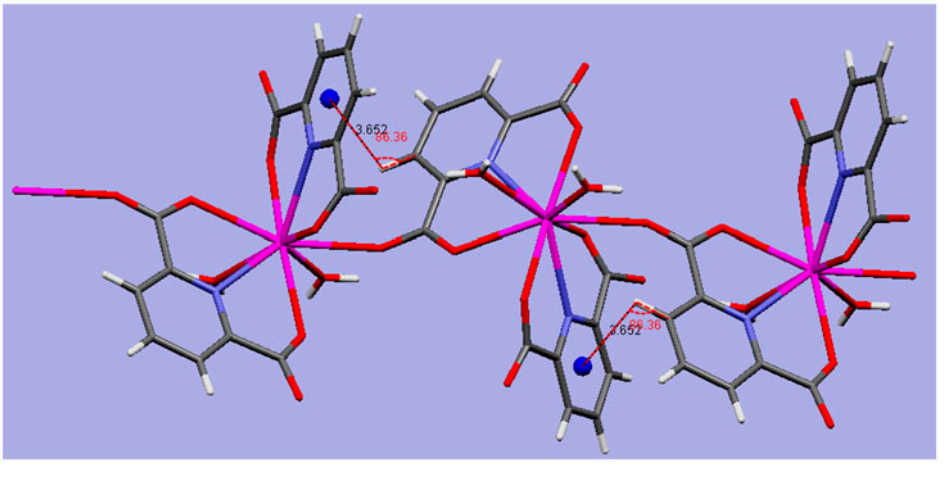

Figure 6. C–H···π stacking between C(9)–H(9A) and pyridine rings (N1, C1–C5) with distance of 3.652 Å and angle value 86.36° in **1**. Cationic fragments and water molecules are omitted for clarity.

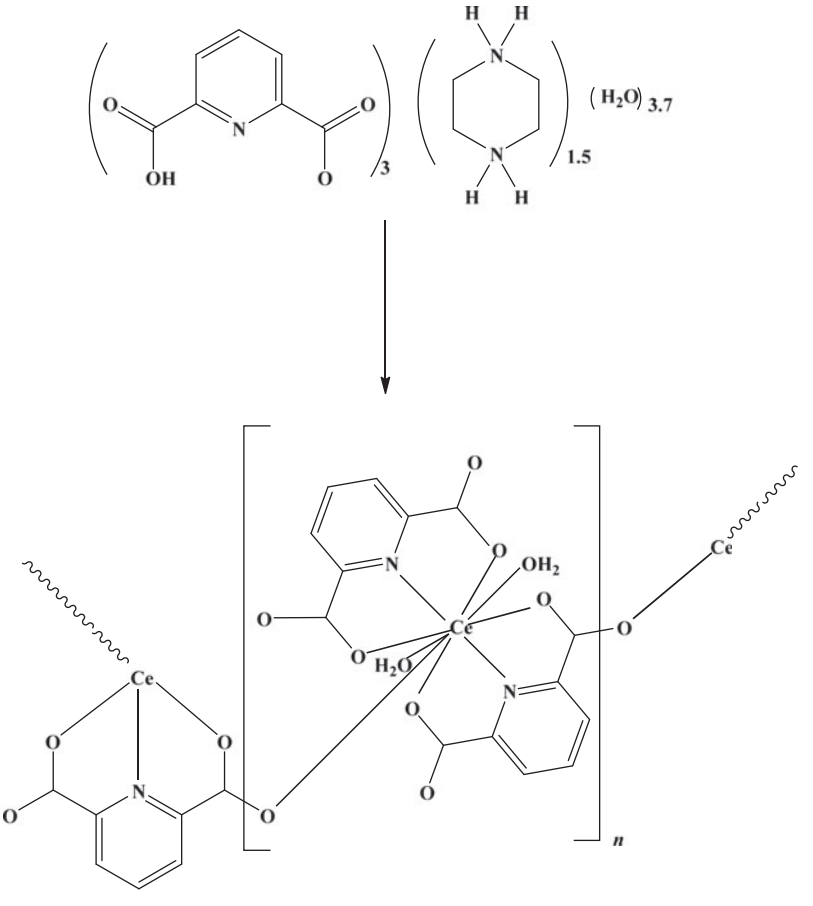

Scheme 2. Synthetic procedure for $[Ce(pydc)_2(H_2O)_2]_n$.

tricapped plane (360.74°) and O–Ce–O bond angles in trigonal prism provide clear evidence for the proposed hypothesis (table 4 and figure 8).

One oxygen of two $(pydc)^{2-}$ plays bridging roles with bond distances of 2.492 Å related to Ce(1)–O(8). The coordination behavior leads to the formation of a ladder-like structure [figure 9(a)]. As can be seen in figure 9(a) and (b), the Ce–pydc–Ce parts are rungs of the ladder, which are alternately repeated in the crystalline network. The ladder structures are connected to each other via hydrogen bonds formed between oxygens of carboxylate, coordinated water, and co-crystallized water [figure 9(b) and (c)].

The waters existing in the unit cell are the coordinated water, which occupies the trigonal prism position in the neutral polymeric complex and four free water molecules. Hydrogen bonds assemble between uncoordinated water and polymeric complex giving an interesting topological motif, which can be depicted as cyclic and chain. In general, O–H···O hydrogen bonds between carboxylate of $(pydc)^{2-}$ moieties and coordinated/uncoordinated water lead to the formation of $R_3^3(8)$, $R_6^4(12)$, and $C_4^4(9)$ hydrogen bonding synthons (figure 10). The two hydrogens of coordinated water (H1 and H4) are engaged in strong hydrogen bonding with oxygen of carboxylate (O3) and of co-crystallized water (O11) as intermolecular

Table 4. Selected bond lengths (Å) and angles (°) of $[Ce(pydc)_2(H_2O)_2]_n \cdot 4H_2O$.

Ce(1)–O(1)	2.5648(16)	Ce(1)–O(7)	2.5530(17)	Ce(1)–O(10)	2.4909(16)
Ce(1)–O(4)	2.4983(16)	Ce(1)–O(8)	2.4920(16)	Ce(1)–N(1)	2.638(2)
Ce(1)–O(5)	2.5325(15)	Ce(1)–O(9)	2.4589(16)	Ce(1)–N(2)	2.6375(18)
O(1)–Ce(1)–O(4)	122.48(6)	O(5)–Ce(1)–O(8)	78.44(5)	O(4)–Ce(1)–N(2)	135.01(5)
O(1)–Ce(1)–O(5)	81.81(5)	O(5)–Ce(1)–O(9)	86.31(6)	O(5)–Ce(1)–N(1)	139.28(5)
O(1)–Ce(1)–O(7)	82.64(5)	O(5)–Ce(1)–O(10)	78.19(6)	O(5)–Ce(1)–N(2)	61.14(5)
O(1)–Ce(1)–O(8)	140.01(5)	O(7)–Ce(1)–O(8)	137.20(5)	O(7)–Ce(1)–N(1)	72.39(6)
O(1)–Ce(1)–O(9)	140.75(5)	O(7)–Ce(1)–O(9)	72.14(6)	O(7)–Ce(1)–N(2)	61.08(5)
O(1)–Ce(1)–O(10)	71.58(5)	O(7)–Ce(1)–O(10)	145.20(6)	O(8)–Ce(1)–N(1)	119.00(6)
O(4)–Ce(1)–O(5)	153.61(5)	O(8)–Ce(1)–O(9)	72.10(5)	O(8)–Ce(1)–N(2)	129.35(5)
O(4)–Ce(1)–O(7)	75.56(5)	O(8)–Ce(1)–O(10)	70.53(5)	O(9)–Ce(1)–N(1)	132.91(6)
O(4)–Ce(1)–O(8)	75.88(5)	O(9)–Ce(1)–O(10)	141.65(5)	O(9)–Ce(1)–N(2)	75.89(6)
O(4)–Ce(1)–O(9)	80.17(6)	O(1)–Ce(1)–N(1)	61.09(5)	O(10)–Ce(1)–N(1)	74.77(6)
O(4)–Ce(1)–O(10)	98.68(6)	O(1)–Ce(1)–N(2)	65.58(5)	O(10)–Ce(1)–N(2)	123.49(6)
O(5)–Ce(1)–O(7)	121.55(5)	O(4)–Ce(1)–N(1)	61.68(5)	N(1)–Ce(1)–N(2)	111.60(6)

Table 5. Intra- and intermolecular hydrogen bonds for $[Ce(pydc)_2(H_2O)_2]_n \cdot 4H_2O$.

D–H	A	d(D–H)	d(H···A)	d(D···A)	<DHA	Symmetry codes
O(9)–H(1)	O(11)	0.85	1.879	2.722(2)	171	x, y, z
O(9)–H(2)	O(12)	0.85	1.894	2.709(2)	160	$-x+2, y+1/2, -z+1/2$
O(10)–H(3)	O(7)	0.85	1.902	2.708(2)	158	$x, -y+3/2, z-1/2$
O(10)–H(4)	O(3)	0.85	1.869	2.704(2)	167	$-x+1, y-1/2, -z+1/2$
O(11)–H(5)	O(5)	0.85	2.032	2.860(2)	164	$x, -y+3/2, z-1/2$
O(11)–H(6)	O(6)	0.85	1.991	2.836(2)	173	$-x+2, -y+1, -z+1$
O(12)–H(7)	O(11)	0.85	2.099	2.853(2)	148	$x, -y+3/2, z-1/2$
O(12)–H(8)	O(6)	0.85	1.859	2.698(2)	169	x, y, z
O(13)–H(9)	O(12)	0.85	2.144	2.993(3)	177	$x, -y+3/2, z-1/2$
O(13)–H(10)	O(4)	0.85	2.102	2.945(3)	171	x, y, z
O(14)–H(11)	O(13)	0.85	1.994	2.763(4)	150	$x, y-1, z$
O(14)–H(12)	O(3)	0.85	1.801	2.640(3)	168	$x, y-1, z$
C(10)–H(10A)	O(11)	0.95	2.580	3.473(3)	156	$-x+2, -y+1, -z+1$

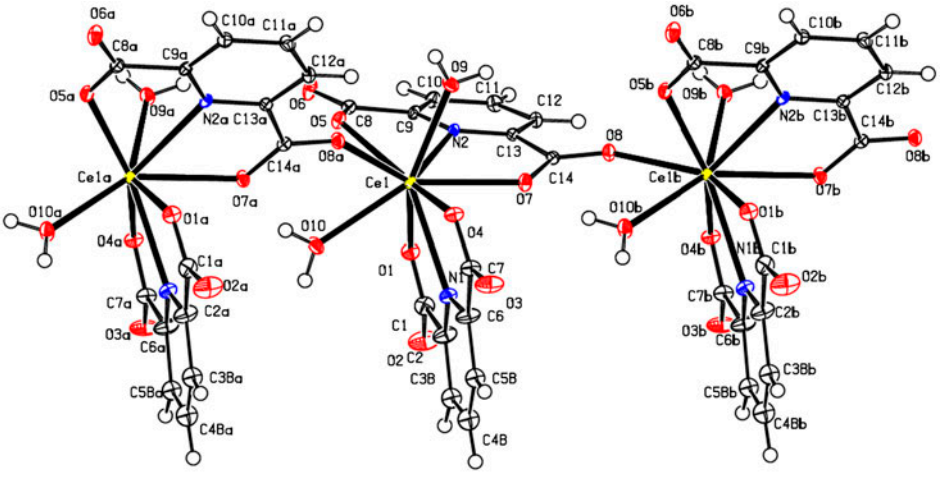

Figure 7. Fragment of $Ce(pydc)_2(H_2O)_2]$ parallel with crystallographic axis *c*. View with thermal ellipsoids given at 50% probability level. Disordered fragment of one pydc anion is dashed.

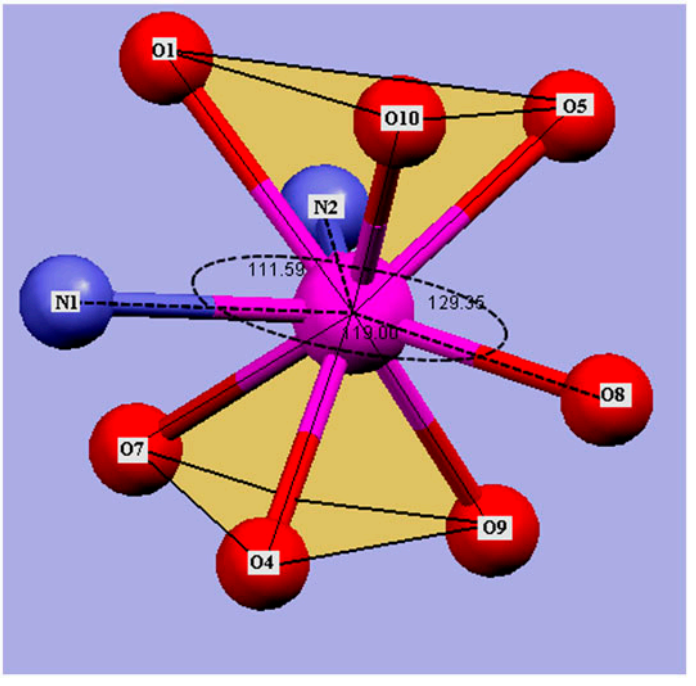

Figure 8. Illustration for coordination environment around Ce^{IV} as distorted tricapped trigonal prism.

interactions (table 5). Also, the strong hydrogen bonding between carboxyl groups of the neutral polymeric complex and water occurs with D···A and H···A distances, and D–H···A angle, 2.836(2) and 1.991 Å, and 173° (table 5). Based on this evidence, strong hydrogen bonds between water molecules were observed in two sets with D···A and H···A distances, and D–H···A angle, 2.993(3) and 2.144 Å, and 177°, and 2.836(2) and 1.991Å, and 173°. Finally, the presence of strong hydrogen bonding of coordinated water and carboxylate, shown in figures 9 and 10, makes the distance close between the each complex. Indeed, van der Waals interactions form the unique supramolecular network in the crystal structure whose water molecules fill the spaces between these ladder-like structures.

The C(8)–O(6)···π (ring: N2,C9–C13) and C(10)–H(10A)···π (ring: N2,C9–C13) stacking interactions between coordinated $(pydc)^{2-}$ from adjacent $[Ce(pydc)_2(H_2O)_2]$ neutral polymeric complex in **2** with distances value of 3.685 and 3.951 Å create the ladder-like structure (figure 11).

3.4. *Solution studies*

The fully protonated forms of pydc (L) and pipz (Q) were titrated with a standard NaOH solution in order to calculate their protonation constants as the building blocks of the pydc–pipz adduct. The protonation constants of pydc [27, 28] and pipz [42] were calculated by fitting the volume–pH data to the BEST program. Evaluation of the equilibrium constants for the interaction of pydc with pipz was accomplished through comparison of the calculated and experimental pH profiles, obtained from mixed pydc–pipz systems [27, 43, 44]. The results of this system were reported previously [45].

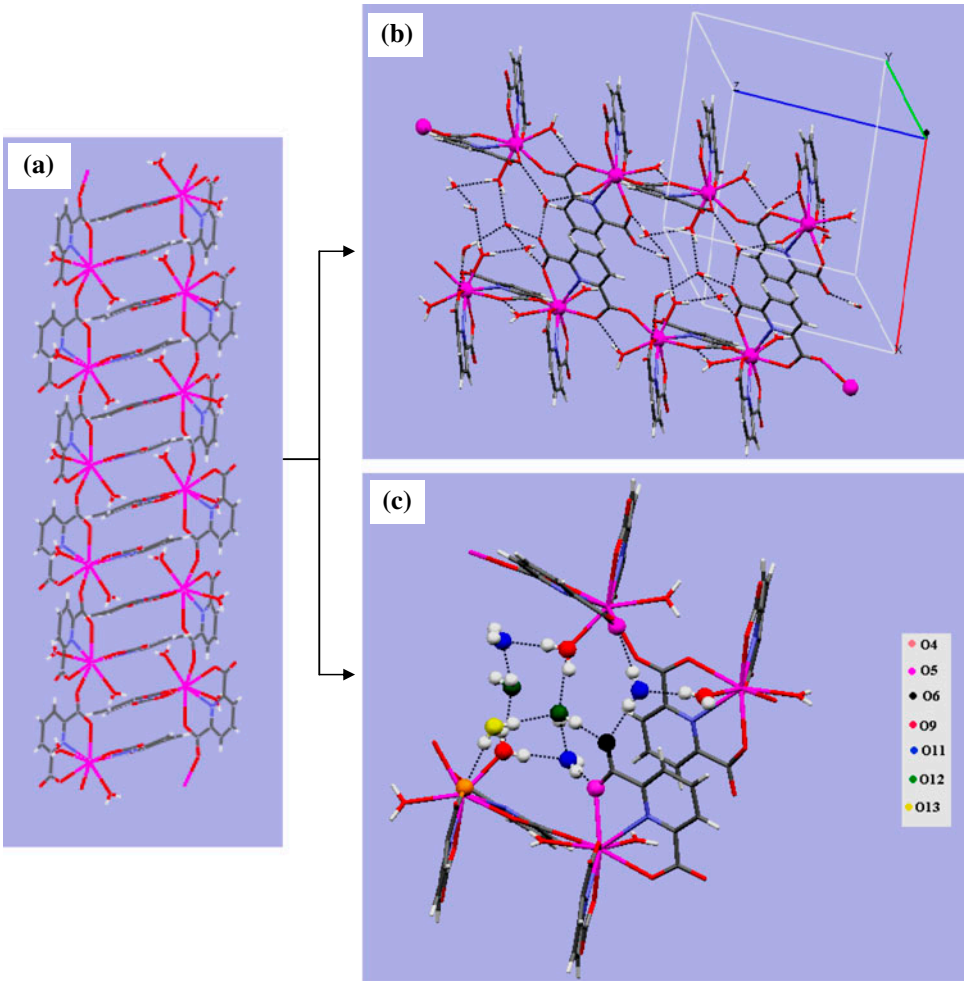

Figure 9. (a) Ladder like structure; (b) hydrogen bonds existing between layers in unit cell; (c) hydrogen bonds between oxygens of carboxylate, coordinated water molecules and co-crystallized water molecules in **2**.

To evaluate the stoichiometry and stability of Sr^{2+} complexes with pydc–pipz salt system in aqueous solution, the equilibrium potentiometric pH titration profiles of pydc [28] and pipz, and their 1 : 1 mixture were obtained in the absence and presence of Sr^{2+} [figures 12(a) and 13(a)]. It is to be noted that the potentiometric pH metric is not a proper method for the investigation of complexation between Ce(IV) and the cited ligands and the corresponding salt system, since Ce(IV) is a relative strong oxidant in solution.

The cumulative stability constants of $M_mL_lQ_qH_h$ and β_{mlqh} were defined in our previous publications [27, 28], where M, L, Q, and H are metal ion, pydc, pipz, and proton, respectively, and m, l, q, and h are the respective stoichiometric coefficients.

The cumulative stability constants were evaluated by fitting the corresponding pH titration curves to the BEST program, and the resulting values for the most likely complex species in aqueous solutions are also included in table 6. The corresponding species distribution diagrams for pydc and pydc–pipz in the presence of Sr^{2+} are shown in figures 12(b) and 13(b).

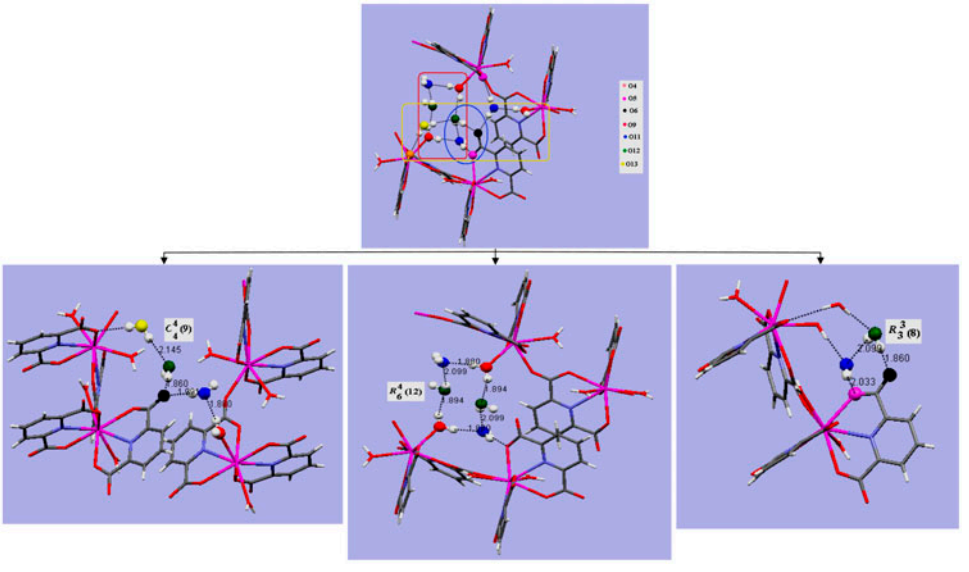

Figure 10. O–H···O Hydrogen bonding interactions between carboxylate moieties and coordinated and/or uncoordinated waters that lead to formation of cyclic and chain hydrogen bonding synthons as $R_3^3(8)$, $R_6^4(12)$ and $C_4^4C_4^4(9)$ in **2**.

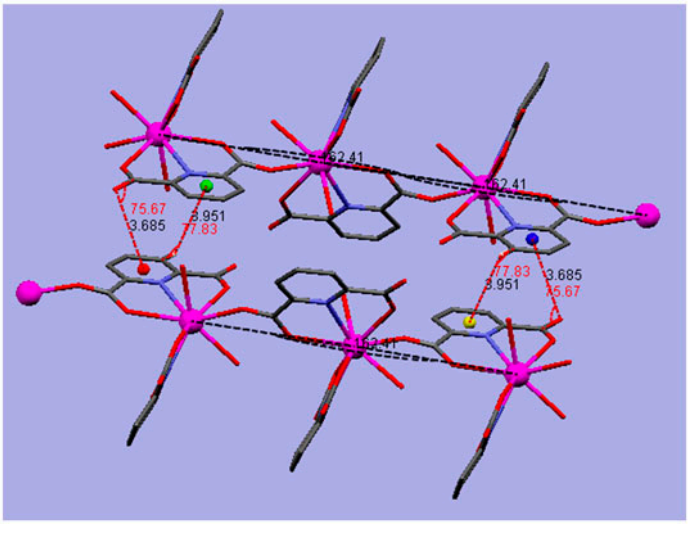

Figure 11. The C(8)–O(6)···π (Ring: N2, C9-C13) and C(10)–H(10A)···π (Ring: N2, C9–C13) stacking interactions between coordinated $(pydc)^{2-}$ ligands from adjacent $[Ce(pydc)_2(H_2O)_2]$ neutral polymeric complexes in **2**.

The observed species and corresponding stability constants of pydc–Sr binary system are shown in table 6. The most likely species are SrLH, SrL_2, and SrL, confirming that no interaction was seen in the binary system between Sr^{2+} and pipz. From figure 13(b) and table 6, it is readily seen that for the pydc–pipz–Sr system, ternary species are $SrLQ_2H$, SrL_2QH_2,

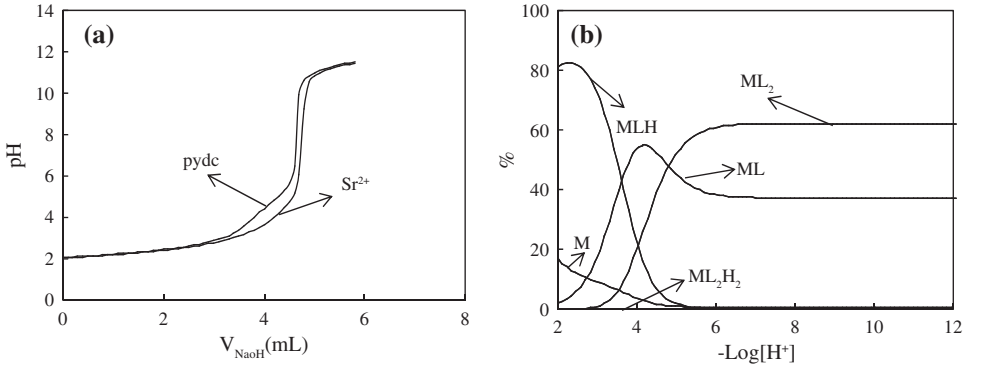

Figure 12. (a) Potentiometric titration curves of pydc in the absence and presence of Sr^{2+} with NaOH 0.10591 M in aqueous solution at 25 °C and $\mu = 0.1$ M $NaNO_3$ and (b) distribution diagrams of binary system pydc(L)/M, M = Sr^{2+}.

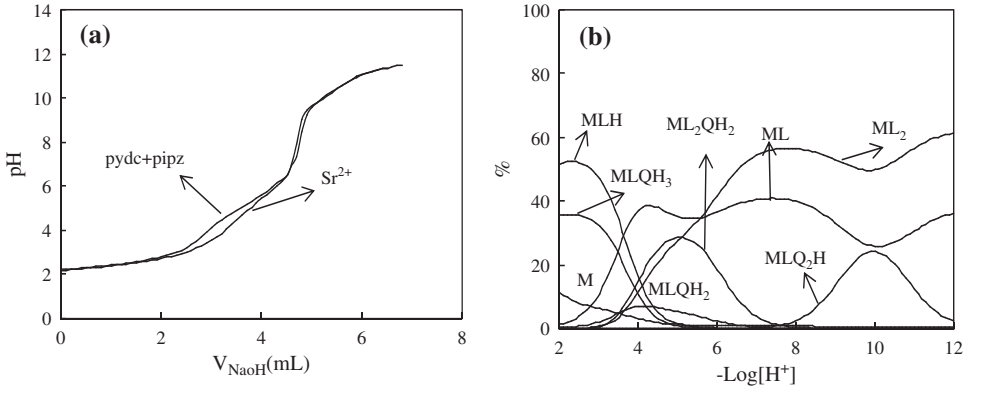

Figure 13. (a) Potentiometric titration curves of pydc + pipz in the absence and presence of M^{2+} with NaOH 0.10591 M in aqueous solution at 25 °C and $\mu = 0.1$ M $NaNO_3$, M = Sr^{2+} and (b) distribution diagrams of pydc (L)/pipz(Q)/M ternary systems, M = Sr^{2+}.

Table 6. Overall stability constants of pipz/pydc/Sr^{2+} (q/l/m) binary and ternary systems in aqueous solution at 25 °C and $\mu = 0.1$ M $NaNO_3$.

System	m	l	q	h	Log β	Max %	at pH
Sr-pydc	1	1	0	0	5.12	54.8	4.2
	1	1	0	1	8.75	82.5	2.36
	1	2	0	0	8.7	62.3	6.8<
	1	2	0	2	12.4	Negligible	–
Sr-pydc-pipz	1	1	1	2	22.74	20.0	4.3
	1	1	1	3	26.92	37.0	2.5>
	1	2	1	2	27.12	28.57	5.0
	1	1	2	1	21.13	24.04	10.0

$SrLQH_2$, and $SrLQH_3$. A comparison between the stoichiometry of the crystalline complex in the pydc–pipz–Sr system, and the results obtained from solution study clearly reveal that SrL_2QH_2 is the most abundant species existing in aqueous solution, possessing a stoichiometry similar to that of the complex obtained in the solid state.

4. Conclusion

Coordination polymers of Sr(II) and Ce(IV) formulated as $(pipzH_2)[Sr(pydc)_2(H_2O)_2]_n{\cdot}4H_2O$ and $[Ce(pydc)_2(H_2O)_2]_n{\cdot}4H_2O$ (pydc = pyridine-2,6-dicarboxylate, pipz = piperazine) were prepared. Synthesis, IR spectroscopy, elemental analysis, structural studies, supramolecular synthons, and potentiometric measurements were investigated. The butterfly- and ladder-like structures of these polymeric complexes are bridged by oxygens of $(pydc)^{2-}$ and M–O(pydc)–M bonds are the rungs for networks. Different non-covalent interactions such as ion-pairing, π-stacking, and hydrogen bonding play important roles in the construction of extended networks in the crystal systems. The stoichiometry of complex species in solution was found to be similar to the cited crystalline metal ion complexes.

Supplementary material

The crystallographic data (structure factors) have been deposited with the Cambridge Crystallographic Data Center (CCDC) as supplementary publication numbers CCDC 634335 and 954343 for **1** and **2**, respectively. These data can be obtained free of charge from the Cambridge Crystallographic Data Center via www.ccdc.cam.ac.uk/data_request/cif.

References

[1] D. Braga. *Chem. Commun.*, 2751 (2003).
[2] E.Q. Gao, Y.F. Yue, S.Q. Bai, Z. He, C.H. Yan. *J. Am. Chem. Soc.*, **126**, 1419 (2004).
[3] M. Oh, G.B. Carpenter, D.A. Sweigart. *Acc. Chem. Res.*, **37**, 1 (2004).
[4] L. Pérez-García, D.B. Amabilino. *Chem. Soc. Rev.*, **31**, 342 (2002).
[5] C.Y. Su, A.M. Goforth, M.D. Smith, P.J. Pellechia, H.C. Zur Loye. *J. Am. Chem. Soc.*, **126**, 3576 (2004).
[6] M. Fujita, Y.J. Kwon, S. Washizu, K. Ogura. *J. Am. Chem. Soc.*, **116**, 1151 (1994).
[7] J.M. Lehn. *Supramolecular Chemistry*, VCH, Weinheim (1995).
[8] S.R. Batten, R. Robson. *Angew. Chem. Int. Ed.*, **37**, 1460 (1998).
[9] P.J. Hagrman, D. Hagrman, J. Zubieta. *Angew. Chem. Int. Ed.*, **38**, 2638 (1999).
[10] D.B. Amabilino, J.F. Stoddart. *Chem. Rev.*, **95**, 2725 (1995).
[11] D.S. Lawrence, T. Jiang, M. Levett. *Chem. Rev.*, **95**, 2229 (1995).
[12] M. Eddaoudi, D.B. Moler, H. Li, B. Chen, T.M. Reineke, M. O'Keeffe, O.M. Yaghi. *Acc. Chem. Res.*, **34**, 319 (2001).
[13] S. Kitagawa, R. Kitaura, S. Noro. *Angew. Chem. Int. Ed.*, **43**, 2334 (2004).
[14] (a) T.L. Hennigar, D.C. MacQuarrie, P. Losier, R.D. Rogers, M.J. Zaworotko. *Angew. Chem. Int. Ed. Engl.*, **36**, 972 (1997); (b) R. Robson. *J. Chem. Soc., Dalton Trans.*, 3735 (2000); (c) L. Carlucci, G. Ciani, D.M. Proserpio. *Coord. Chem. Rev.*, **246**, 247 (2003); (d) O.M. Yaghi, M. O'Keeffe, N.W. Ockwig, H.K. Chae, M. Eddaoudi, J. Kim. *Nature*, **423**, 705 (2003); (e) D. Bradshaw, T.J. Prior, E.J. Cussen, J.B. Claridge, M.J. Rosseinsky. *J. Am. Chem. Soc.*, **126**, 6106 (2004); (f) S. Kitagawa, R. Kitaura, S. Noro. *Angew. Chem. Int. Ed.*, **43**, 2334 (2004).
[15] (a) S.R. Batten, R. Robson. *Angew. Chem. Int. Ed.*, **37**, 1460 (1998); (b) K.S. Min, M.P. Suh. *J. Am. Chem. Soc.*, **122**, 6834 (2000); (c) B. Moulton, M. Zaworotko. *J. Chem. Rev.*, **101**, 1629 (2001); (d) M.E. Davis. *Nature*, **417**, 813 (2002); (e) L. Carlucci, G. Ciani, D.M. Proserpio, F. Porta. *Angew. Chem. Int. Ed.*, **42**, 317

(2003); (f) J.L.C. Rowsell, A.R. Millward, K.S. Park, O.M. Yaghi. *J. Am. Chem. Soc.*, **126**, 5666 (2004); (g) X.M. Chen, G.F. Liu. *Chem. Eur. J.*, **8**, 4811 (2002).
[16] (a) M.L. Tong, S. Hu, J. Wang, S. Kitagawa, S.W. Ng. *Cryst. Growth Des.*, **5**, 837 (2005); (b) B. Zhao, L. Yi, Y. Dai, X.Y. Chen, P. Cheng, D.Z. Liao, S.P. Yan, Z.H. Jiang. *Inorg. Chem.*, **44**, 911 (2005); (c) L. Pan, T. Frydel, M.B. Sander, X. Huang, J. Li. *Inorg. Chem.*, **40**, 1271 (2001).
[17] S. Sheshmani, M. Ghadermazi, E. Motieiyan, A. Shokrollahi, Z. Malekhosseini, M. Arab Fashapoyeh. *J. Coord. Chem.*, **66**, 3949 (2013).
[18] W.G. Lu, L. Jiang, X.L. Feng, T.B. Lu. *Cryst. Growth Des.*, **6**, 564 (2006).
[19] N.N. Golovnev, M.S. Molokeev, S.N. Vereshchagin, V.V. Atuchin. *J. Coord. Chem.*, **66**, 4119 (2013).
[20] I.U. Khan, S. Sharif, O. Sahin. *J. Coord. Chem.*, **66**, 3113 (2013).
[21] M.L. Chen, Y.H. Hou, W.S. Xia, Z.H. Zhou. *J. Coord. Chem.*, **66**, 1906 (2013).
[22] M. Zhu, W. Fu, G. Zou. *J. Coord. Chem.*, **65**, 4108 (2012).
[23] S. Sharif, O. Sahin, I.U. Khan, O. Buyukgungor. *J. Coord. Chem.*, **65**, 1892 (2012).
[24] L.D. Wang, F. Tao, M.L. Cheng, Q. Liu, W. Han, Y.J. Wu, D.D. Yang, L.J. Wang. *J. Coord. Chem.*, **65**, 923 (2012).
[25] Bruker. *APEX2 Software Package*, Bruker AXS Inc., Madison, WI (2005).
[26] G.M. Sheldrick. *SHELXTL (v. 5.10)*, *Structure Determination Software Suite*, Bruker AXS, Madison, WI (1998).
[27] A. Moghimi, S. Sheshmani, A. Shokrollahi, M. Shamsipur, G. Kickelbik, H. Aghabozorg. *Z. Anorg. Allg. Chem.*, **631**, 160 (2005).
[28] H. Aghabozorg, F. Ramezanipour, J. Soleimannejad, M.A. Sharif, A. Shokrollahi, M. Shamsipur, A. Moghimi, J. Attar Gharamaleki, V. Lippolis, A.J. Blake. *Polish J. Chem.*, **82**, 487 (2008).
[29] Z. Aghajani, H. Aghabozorg, E. Sadr-Khanlou, A. Shokrollahi, S. Derki, M. Shamsipur. *J. Iran. Chem. Soc.*, **6**, 373 (2009).
[30] A. Shokrollahi, M. Ghaedi, H.R. Rajabi, M.S. Niband. *Spectrochim. Acta, Part A*, **71**, 655 (2008).
[31] A.E. Martell, R.J. Motekaitis. *Determination and Use of Stability Constants*, 2nd Edn, pp. 143–172, VCH, New York (1992).
[32] H. Aghabozorg, E. Motieiyan, A.R. Salimi, M. Mirzaei, F. Manteghi, A. Shokrollahi, S. Derki, M. Ghadermazi, S. Sheshmani, H. Eshtiagh-Hosseini. *Polyhedron*, **29**, 1453 (2010).
[33] A. Chandramohan, R. Bharathikannan, M.A. Kandhaswamy, J. Chandrasekaran, V. Kandavelu. *Cryst. Res. Technol.*, **43**, 93 (2008).
[34] F. Ramezanipour, H. Aghabozorg, A. Shokrollahi, M. Shamsipur, H. Stoeckli-Evans, J. Soleimannejad, S. Sheshmani. *J. Mol. Struct.*, **779**, 77 (2005).
[35] K. Nakamoto. *Infrared and Raman Spectra of Inorganic and Coordination Compounds, Part B*, 5th Edn, Wiley, New York (1997).
[36] H. Aghabozorg, M. Ghadermazi, B. Nakhjavan, F. Manteghi. *J. Chem. Crystallogr.*, **38**, 135 (2008).
[37] A. Moghimi, S.M. Moosavi, D. Kordestani, B. Maddah, M. Shamsipur, H. Aghabozorg, F. Ramezanipour, G. Kickelbick. *J. Mol. Struct.*, **828**, 38 (2007).
[38] I. Ucar, B. Karabulut, A. Bulut, O. Büyükgüngör. *J. Mol. Struct.*, **336**, 834 (2007).
[39] K. Jayaraman, A. Choudhury, C.N.R. Rao. *Solid State Sci.*, **4**, 413 (2002).
[40] M. Singh, S.E. Lofland, K.V. Ramanujachary, A. Ramanan. *Cryst. Growth Des.*, **10**, 5101 (2010).
[41] K. Pavani, M. Singh, A. Ramanan. *Aust. J. Chem.*, **64**, 68 (2011).
[42] H. Aghabozorg, F. Mahfoozi, M.A. Sharif, A. Shokrollahi, S. Derki, M. Shamsipur, H.R. Khavasi. *J. Iran. Chem. Soc.*, **7**, 727 (2010).
[43] B. English, A.E. Martell, R.J. Motekaitis, I. Murase. *Inorg. Chim. Acta*, **258**, 183 (1997).
[44] M.A. Sharif, H. Aghabozorg, A. Shokrollahi, G. Kickelbick, A. Moghimi, M. Shamsipur. *Polish J. Chem.*, **80**, 847 (2006).
[45] H. Aghabozorg, F. Manteghi, M. Ghadermazi, M. Mirzaei, A.R. Salimi, A. Shokrollahi, S. Derki, H. Eshtiagh-Hosseini. *J. Mol. Struct.*, **919**, 381 (2009).